

Near-threshold properties of the electronic density of layered quantum-dots

Alejandro Ferrón,^{1,*} Pablo Serra,^{2,†} and Omar Osenda^{2,‡}

¹*Instituto de Modelado e Innovación Tecnológica (CONICET-UNNE),
Avenida Libertad 5400, W3404AAS Corrientes, Argentina*

²*Facultad de Matemática, Astronomía y Física,
Universidad Nacional de Córdoba and IFEG-CONICET,
Ciudad Universitaria, X5016LAE Córdoba, Argentina*

(Dated: October 28, 2018)

Abstract

We present a way to manipulate an electron trapped in a layered quantum dot based on near-threshold properties of one-body potentials. Firstly, we show that potentials with a simple global parameter allows the manipulation of the wave function changing its spatial localization. This phenomenon seems to be fairly general and could be implemented using current quantum-dot quantum wells technologies and materials if a proper layered quantum dot is designed. So, we propose a model layered quantum dot that consists of a spherical core surrounded by successive layers of different materials. The number of layers and the constituent material are chosen to highlight the near-threshold properties. The manipulation of the spatial localization of the electron in a layered quantum dot results consistent with actual experimental parameters.

PACS numbers: 73.22.-f,73.22.Dj

I. INTRODUCTION

The tailoring of particular quantum states has become an usual task in quantum information processing¹. Semiconductor quantum dots (QDs) are ideally suited to storage quantum information through its eigenstates, since electrons in QDs can store quantum phase coherence for very long periods of time². In addition the amount of entanglement that a multi-electron QD can keep in storage could be useful to implement quantum information tasks, but there exist very few examples of ab initio calculations that attempt to quantify it in the literature³⁻⁸. The dots can be designed in a host of ways to meet the specific requirements of the quantum information task in sight, by choosing its shape, size or materials⁹.

On the other hand, the advances in semiconductor technology allow the preparation of more complex structures than the simple quantum well. Between the more complex structures, the quantum-dot quantum wells structures¹⁰ and multiple quantum rings¹¹ have been extensively studied. The quantum-dot quantum wells (QDQW's) structures are multi-layered quantum dots, composed of two semiconductor materials, the one with the smaller bulk band gap is sandwiched between a core and an outer shell of the material with larger bulk band gap. Because of its properties, the QDQW's have been demonstrated to form an efficient gain medium for nanocrystal-based lasers¹², and its electronic structure has been obtained from first-principles calculations¹³. It is remarkable that the effective mass approximation (EMA) seems to predict fairly well the behavior of the electronic density¹³⁻¹⁵ when compared with first-principles calculations.

The quantum ring structures are an ideal playground to study many subtle quantum phenomena as the Aharonov-Bohm effect¹⁶ which leads to the presence of persistent currents¹⁷. This persistent currents have been measured even for one electron states¹⁸. The quantum rings are formed by only one semiconductor material, and the fabrication of multiple concentric quantum rings (up to five) can be achieved with high quality and reliability¹⁹.

Despite all the advantages that quantum dots present as implementations of physical qubits, the confined electrons interact with thousands of spin nuclei through the hyperfine interaction. This leads, inevitably, to decoherence. To solve the decoherence problem it has been proposed that the physical qubit should be implemented by two electrons confined in a double quantum dot²⁰. The coupling of the two quantum dots depends on the spatial extent

of the one-electron wave functions, in particular it determines the strength of the exchange interaction between the two electrons. The exchange coupling in double quantum dots has been studied extensively, in particular how it can be tuned using electric fields²¹, magnetic fields²³, or the effect of the confinement of the double quantum dot in a quantum wire²². So, the ability to manipulate the spatial extent of the one electron wave function in an isolated QD, can be decisive when dealing with the states of a double quantum dot.

In addition, the recent advances in materials manipulation at the nanoscale allow an accurate shape and size control of the QD that offers the possibility of tailoring the energy spectrum to produce desirable optical transitions. These tasks are useful for the development of optical devices with tunable emission or transmission properties. Optical properties of artificial molecules and atoms are subject of great interest because of their technological implementations. In spherical QD, the optical properties such as the dipole transition, the oscillator strength and the photoionization cross section have been studied theoretically by different authors²⁴⁻²⁹.

In this work we present a way to manipulate the wave function of an electron trapped in a quantum dot whose energy is near the continuous threshold. The phenomena associated seem to be fairly general and could be implemented using current quantum-dot quantum wells technologies and materials. In particular we show that the phenomenon is present in a layered quantum dot model whose parameters are consistent with actual experimental values.

The paper is organized as follows. In Sec. II we introduce a simple model whose near-threshold behavior shows how the localization of the ground state electronic density could be handled easily. In Sec. III we apply the findings of Section II to design a QDQW-like model that is both consistent with actual experimental values and able to exploit the near-threshold phenomenon. Here we perform calculations for the ground state and the first excited p state, and we analyze the optical properties of the model. Finally, Sec. IV contains the conclusions with a discussion of the most relevant points of our findings.

II. ONE ELECTRON OSCILLATING POTENTIAL

In this section we report results for the ground state electronic density of one electron in an oscillating short range potential. The near threshold properties will be exploited in

the next Section to design quantum dot structures. We choose an smooth and analytical potential to emphasize that the behavior of the electronic density is fairly general. The one particle Hamiltonian is given by

$$H = -\frac{\hbar^2}{2m}\nabla^2 + W(r), \quad (1)$$

where

$$W(r) = -W_0 e^{-\gamma r} \sin(\omega r), \quad (2)$$

where W_0 is the strength of the potential and γ and ω are positive constants. Clearly, the potential well range is given by γ and the number of spherical layers and their width are related to ω . The successive spherical layers are similar to a succession of potential wells and barriers.

It is known that for fixed values of γ and ω , there is a critical value $W_0^{(c)}$ such that the Hamiltonian Eq. (1) supports at least one bound state only if $W_0 > W_0^{(c)}$ ³². In the following, we will study the near-threshold properties of the ground state electronic density varying W_0 as a global parameter, for $W_0 \gtrsim W_0^{(c)}$.

The ground state energy and wave function of Hamiltonian Eq. (1) were obtained numerically, using the fourth-order Runge-Kutta method for the potential in Eq. 2. The electronic density, $\rho(r)$, is given by

$$\rho(r) = \int |\Psi(\mathbf{r})|^2 r^2 d\Omega, \quad (3)$$

where Ψ is the one-electron wave function. We are interested in the probability of finding the electron in the n -th well. Figure 1 shows the electronic density $\rho(r)$ for different values of W_0 . By changing the value of W_0 it is possible to select in which potential well the maximum value of the electronic density is located. The particular value of W_0 that locates the maximum of the electronic density in, say, the third well depends on the actual values of γ and ω .

In Figure 2a we can observe the position where the electronic density achieves its maximum value (r_{max}). We can check that the value r_{max} is rather stable as a function of W_0 . Moreover, Figure 2a shows that changing W_0 allows selecting in which well the electronic density will have its maximum value. It is worth to mention that this effect is a near-threshold phenomenon different from those reported previously in the literature for

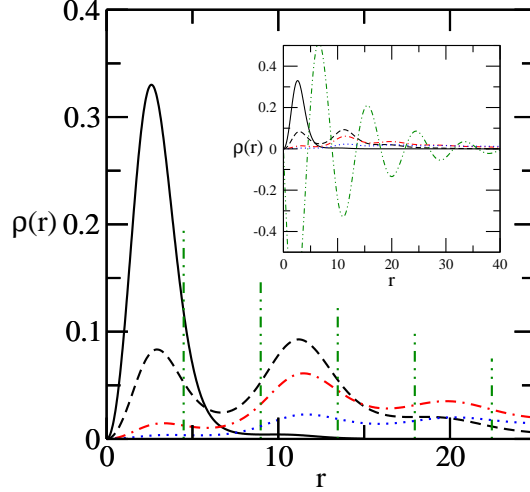


FIG. 1. (color on-line) Electronic density as a function of r for the ground state Hamiltonian (Eq. (1)). The dark green vertical dashed dotted lines show the zeros of the potential defined in Eq. (2). The black continuous line shows the electronic density for $W_0 = 0.3 a.u.$, the black dashed line shows the electronic density for $W_0 = 0.2 a.u.$, red dashed dotted line shows calculation for $W_0 = 0.16 a.u.$ and blue dotted line shows the electronic density for $W_0 = 0.14 a.u.$ The inset shows the same electronic densities and the potential in a different scale. The dark green dashed dotted curve corresponds to the potential, which is plotted in W_0 units.

electrons localized in complex nanostructures^{10,23}, since in our example the maximum is not necessarily located in the deepest well.

The maximum in the electronic density as a function of the strength potential shows an interesting phenomenon. We can observe how this maximum jumps from a well to the next well when the strength potential is continuously varied. It is important to note that we have a situation where the maximum is not located in the deepest well. In order to clarify this phenomenon we define the “well occupation probability”,

$$I_n = \int_{2(n-1)\pi/\omega}^{(2n-1)\pi/\omega} \rho(r) dr \quad (4)$$

that allows us to evaluate how much of the electronic density is in the n -th well. In figure 2b we show the numerical calculations of I_n for different values of n . The intersection of the black solid line (I_1) and the red dashed line (I_2), of Figure 2b, give us the value of W_0 where a qualitatively change in the electronic density occurs. For this value of W_0 we have the first

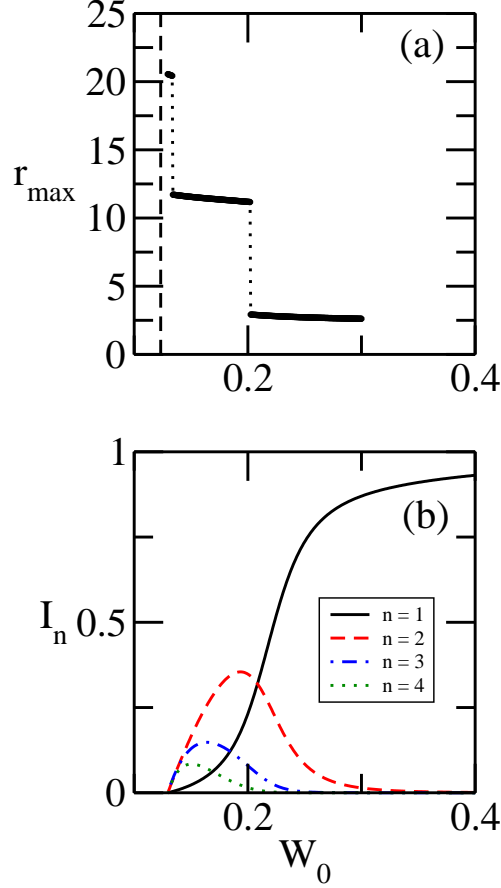


FIG. 2. (color on-line) (a) Position where the electronic density achieves its maximum value (r_{\max}) as a function of W_0 . The vertical dashed line shows the critical ionization value, $W_0^{(c)}$. (b) The well occupation probability, I_n , as a function of W_0 . For large values of W_0 the ground state wave function is localized around the origin, so only I_1 is appreciable. For smaller values of W_0 , I_1 drops to zero and the successive wells became occupied. Near the threshold many wells are occupied but $I_n \rightarrow 0, \forall n$.

jump. The second jump occurs for the value of W_0 where the red dashed line and the blue dashed dotted line intersect.

Finally in Figure 3 we plot the Contour map of the electronic density as a function of the coordinate r and the strength potential W_0 for the potential defined in Eq. (2). Here we can appreciate clearly the effect reported in this work. For larger values of W_0 ($W_0 > 0.25$) the electronic density presents just one peak located in the first well. When we decrease the value of W_0 we start to see a second (lower) peak located in the second well, but for values

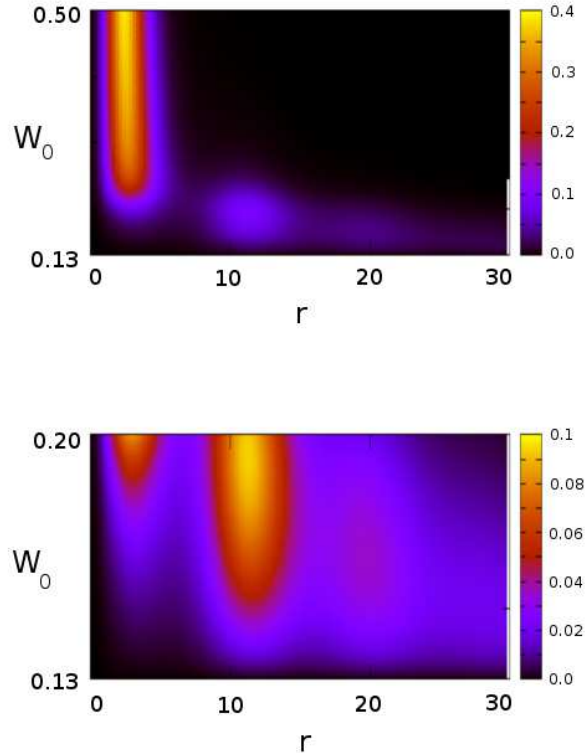


FIG. 3. (color on-line) The upper panel shows the contour map of the electronic density as a function of the coordinate r and the strength potential W_0 for the potential defined in Eq. (2). A zoom of this figure is shown in the lower panel. The figures show how the electronic density's higher peak moves as W_0 decreases. Note that for certain values of W_0 the electronic density has one, two or three peaks.

of $W_0 \simeq 0.2$ the second peak is higher than the first peak and the maximum is not located in the deepest well. If we continue decreasing W_0 the peak in the first well vanishes and we start to appreciate a new peak in the third well.

III. ONE ELECTRON QDQW-LIKE MODEL

The ability to produce easily distinguishable quantum states in nanodevices is of fundamental importance because of its potential technological applications, in this sense we show that the spatial extent of the ground state electronic density can be noticeably changed,

without changing the spatial extent of the nanostructure. The ground states could be distinguished by current imaging techniques³¹.

On the following we show how our findings could be relevant in actual physical implementations. The synthesis of layered quantum dots is a well known technique, see Reference¹⁰ and references therein. Moreover, the EMA approximation appropriately describes the electronic structure of nanostructures formed by layers of CdS and HgS. Since the modulation of a global parameter like our W_0 is not easily achievable, and that the potential well in CdS/HgS compounds is given by the conduction band offset between the two materials, the only parameters that can be varied with some ease by experimentalist are the width and the materials of the layers. Another difference when dealing with hetero nanostructures with the simple model Hamiltonian in Eq. (1) results from the different effective mass characteristic of each material.

Here we consider structures with two wells made of a HgS layer, separated by one CdS step and with a central CdS core. The step-like potential can be written

$$V(r) = \begin{cases} V_0, & r < r_c; (CdS), \\ 0, & r_c \leq r < r_1; (HgS), \\ V_0, & r_1 \leq r < r_2; (CdS), \\ 0, & r_2 \leq r < r_3; (HgS), \\ V_0, & r \geq r_3; (CdS). \end{cases} \quad (5)$$

where the potential well depth is $V_0 = 1.35 \text{ eV}$, which corresponds to the band offset between CdS and HgS, while the effective masses are $0.2m_e$ and $0.036m_e$ respectively³³. The width of the inner and outer HgS layers were fixed equal to 2 and 1.5 nm, respectively, while the width of CdS layer that separates them was fixed to 2 nm. The width of the central CdS core is going to be varied in order to show the phenomenon presented in previous section. An important difference with W_0 is that the width of the layers can be varied easily in the laboratory.

A. Ground state electronic density

Here we evaluate the ground state electronic density for the layered QD given by Equation (5), as we did it in the previous section.

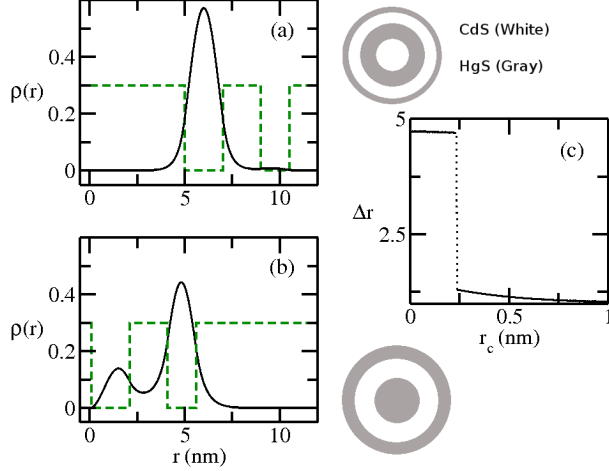


FIG. 4. (color on-line) The electronic density for two different layered quantum dots. The electronic density in panel (a) corresponds to a CdS/HgS/CdS/HgS/CdS structure ($r_c = 2 \text{ nm}$), while panel (b) corresponds to a HgS/CdS/HgS/CdS one ($r_c = 0 \text{ nm}$). The structures are shown as ring patterns (after the last HgS layer we consider that we have a very long CdS barrier). The panel (c) shows the behavior of the position where the electronic densities achieves its maximum value ($\Delta r = r_{max} - r_c$), measured with respect to the inner radius of the first potential well as a function of the core width r_c . For large enough values of the CdS core the electronic density maximum lies in the first potential well, as shown in the panel (a). When the radius of the CdS core approaches 0.5 nm the maximum of the electronic density jumps to the second potential well, as shown by the abrupt change in Δr in panel (c). The blue dashed line in (a) and (b) shows the step like potential.

As Figure 4 shows, by changing the width of the CdS core the electronic density maximum can be located in the potential well of election. Besides, the position of the maximum, as a function of the core width, shows the same behavior that the electronic density of the model Hamiltonian, compare the Figure 4c with Figure 2a.

The stability of the electronic density's maximum can be used when dealing with coupled structures. The fabrication of nanodevices is subjected to many errors so, at least in principle, it could be very useful to have nano-structures whose properties are not excessively sensitive to the actual fabrication parameters.

B. Optical Properties

Optical properties are related to the transitions between different states of the quantum system. In this section we need to evaluate the ground state and some of the excited states of the one electron system. As we mentioned before, the phenomenon under investigation is a near threshold property of the system, because of that, the calculation of the excited states requires some effort.

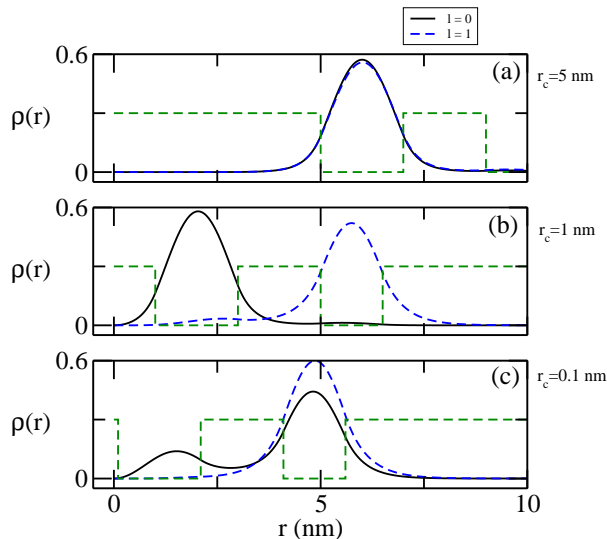


FIG. 5. (color on-line) The electronic density for three different CdS/HgS/CdS/HgS/CdS layered quantum dots. The electronic density in panel (a) corresponds to $r_c = 5\text{ nm}$, while panel (b) $r_c = 1\text{ nm}$ and panel (c) $r_c = 0.1\text{ nm}$. The dark green dashed line in (a), (b) and (c) shows the step like potential.

In Figure 5 we show the electronic densities for the ground state and the lower excited state with angular momentum $l = 1$. In Figure 5 (a) we can see that the maximum of both electronic densities are located in the first potential well. As we decrease the width of the central core (r_c) we observe that the maximum value of the excited state electronic density jumps to the second potential well while the ground state electronic density remains almost unchanged (Figure 5 (b)). Finally, for small values of the central CdS core we obtain the picture presented before. In Figure 5 (c) we can see that the maximum of both electronic densities ($l = 0$ and $l = 1$) are located in the second potential well. It is reasonable to assume that this issue must be reflected in the transition rates between these states, and

therefore in the optical properties of the one electron QDQW.

It is worth to mention that the overlap between the ground state and the excited p state varies from almost one (see Figure 5a) to a very small value (see Figure 5b), and back (see Figure 5c), without changing very much the size of the device. This feature can not be achieved with single well QD without changing its size over one or two magnitude orders since for very large QD the eigenfunctions become very delocalized, resulting in a large overlap between them.

In order to analyze the optical properties of the one electron layered quantum-dots we are going to investigate the electronic dipole-allowed transitions. With this purpose we calculate the Oscillator Strength P_{fi} that is a dimensionless quantity that can be evaluated using the expression³⁴

$$P_{fi} = C\Delta E_{fi}|M_{fi}|^2, \quad (6)$$

where M_{fi} is the dipole transition matrix element between the lower (i) state and the upper state (f), $\Delta E_{fi} = E_f - E_i$ and C is a normalization constant. Using the Thomas-Reiche-Kuhn sum rule

$$\sum_n P_{0n} + \int_0^\infty P_{0E}dE = 1, \quad (7)$$

the normalization constant can be calculated as

$$C = \left\langle 0 \left| \frac{1}{m^*(r)} \right| 0 \right\rangle^{-1}. \quad (8)$$

In Figure 6a we can observe the oscillator strength for the transitions between the ground state and the lower excited state with $l = 1$ as a function of the core width. In the lower panel, Figure 6b we show, as in Figure 4(c), the behavior of the position where the electronic densities (ground and excited states) achieves its maximum value ($\Delta r = r_{max} - r_c$), measured with respect to the inner radius of the first potential well as a function of the core width r_c . For large enough values of the CdS core the electronic density maximums lie in the first potential well. As the radius of the CdS core decreases the maximums of the electronic densities jumps to the second potential well ($r_c = 1.8nm$ for the excited state density and $r_c = 0.23nm$ for the ground state density), as shown by the abrupt change in Δr . As we can see in the inset of Figure 6a the oscillator strength rapidly decrease for large values of

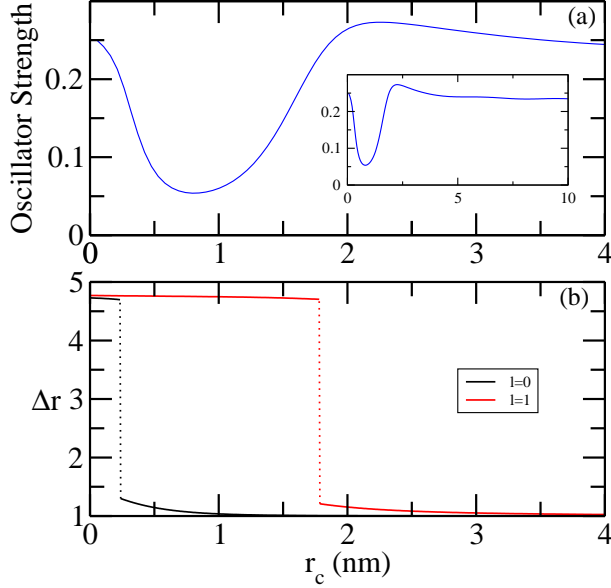


FIG. 6. (color on-line) Panel (a) shows the oscillator strength as a function of the core width r_c calculated using Equation (6) for the ground and lower excited state with $l = 1$. Panel (b) shows the behavior of the position where the electronic densities achieves its maximum value ($\Delta r = r_{max} - r_c$), measured with respect to the inner radius of the first potential well as a function of the core width r_c . For large enough values of the CdS core the electronic density maximums lie in the first potential well. When the radius of the CdS core approaches 1.8 nm (0.23 nm) the maximum of the excited state (ground state) electronic density jumps to the second potential well, as shown by the abrupt change in Δr .

the width of the central CdS core and then reaches to a limit value. The behavior for small values of r_c is rather more complicated, and as was pointed out before, the phenomenon becomes evident. It is clear from Figure 6a and Figure 6b that when the maximum values of the electronic densities are located in different potential wells, the oscillator strength presents a dramatic decrease.

IV. CONCLUSIONS

We have shown a complete analysis of the ground state of one electron in a spherical potential described in Eq. (2) and (5). We find a effect that, to the best of our knowledge, has not been reported in the literature. For the potential defined in (5) we analyzed the

ground and the lower excited state with $l = 1$. The effect mentioned before is also present in the excited state. We finished the present work with the study of the optical properties of the one electron layered quantum-dots. Here we find that the effect is detected by the oscillator strength, that is a very important physical quantity in the study of the optical properties, and is related to the electronic dipole-allowed transitions. Moreover, we can conclude that we can have a great control of the optical properties of these nanostructures in a simple manner using the well known techniques of synthesis of layered quantum dots. A small change in the width of the central core can produce dramatic changes in the optical properties of QDQW.

This phenomenon can be experimentally observed with the actual semiconductor technology. One possible setback for the observation of the phenomenon discussed in this work comes from the low binding energies associated to near-threshold phenomena. Given the fairly simple dependence of the reported phenomenon on the potential characteristics, we believe that its observation is possible and feasible. For the model analyzed in this paper, the availability of materials with larger band offsets could render the phenomenon more pronounced and with larger eigenenergies.

The behavior of the electronic density in one and two dimensional systems with a potential equivalent to Eq. (2) is qualitatively the same. Anyway, since the near-threshold behavior in two dimension is not exactly the same that the observed in three dimensions, it is possible that the jumping of the electronic density between 2-D potential wells could be observed more easily than in the three dimensional case. On the other hand, since in near-threshold two-dimensional systems the wave function rapidly spreads over very large regions, a delicate trade-off between the localization and delocalization could take place.

Other possible extension of our problem to be studied, is its appearance in electrostatic quantum dots³⁵.

ACKNOWLEDGMENTS

We would like to acknowledge SECYT-UNC, CONICET and MinCyT Córdoba for partial financial support of this project.

* aferron@conicet.gov.ar

† serra@famaf.unc.edu.ar

‡ osenda@famaf.unc.edu.ar

- ¹ R. Brunner, Y.-S. Shin, T. Obata, M. Pioro-Ladrière, T. Kubo, K. Yoshida, T. Taniyama, Y. Tokura, and S. Tarucha, *Phys. Rev. Lett.* **107**, 146801 (2011).
- ² R. Takahashi, K. Kono, S. Tarucha, and K. Ono, *Phys. Rev. Lett.* **107**, 026602 (2011).
- ³ A. Ferrón, O. Osenda and P. Serra, *Phys. Rev. A* **79**, 032509 (2009).
- ⁴ F. M. Pont, O. Osenda, J. H. Toloza and P. Serra *Phys. Rev. A* **81**, 042518 (2010).
- ⁵ F. M. Pont, O. Osenda, and P. Serra, *Phys. Scr.* **82**, 038104 (2010).
- ⁶ M. Bylicki, W. Jaskólski, A. Stachów, and J. Diaz, *Phys. Rev. B* **72**, 075434 (2005).
- ⁷ J. P. Coe, and I D'Amico *J. Phys.:* Conf. Ser. **254**, 012010 (2010).
- ⁸ S. Abdullah, J. P. Coe, and I D'Amico *Phys. Rev. B* **80**, 235302 (2009)
- ⁹ Stephanie M. Reimann and Matti Manninen, *Rev. Mod. Phys.* **74**, 1283 (2002)
- ¹⁰ D. Schooss, A. Mews, A. Eychmüller, and H. Weller, *Phys. Rev. B* **49**, 17072 (1994).
- ¹¹ Takaaki Mano, Takashi Kuroda, Stefano Sanguinetti, Tetsuyuki Ochiai, Takahiro Tateno, Jongsu Kim, Takeshi Noda, Mitsuo Kawabe, Kazuaki Sakoda, Giyuu Kido, and Nobuyuki Koguchi, *NANO LETTERS* **5**, 425 (2005).
- ¹² J. Xu and M. Xiao, *Appl. Phys. Lett.* **87**, 173117 (2005).
- ¹³ Joshua Schrier and Lin-Wang Wang, *Phys. Rev. B* **73**, 245332 (2006)
- ¹⁴ J. Berezovsky, M. Ouyang, F. Meier, D. D. Awschalom, D. Battaglia, and X. Peng, *Phys. Rev. B* **71**, 081309(R) (2005).
- ¹⁵ F. Meier and D. D. Awschalom, *Phys. Rev. B* **71**, 205315 (2005)
- ¹⁶ M. Bayer, M. Korkusinski, P. Hawrylak, T. Gutbrod, M. Michel, and A. Forchel, *Phys. Rev. Lett.* **90**, 186801 (2003)
- ¹⁷ D. Mailly, C. Chapelier, and A. Benoit, *Phys. Rev. Lett.* **70**, 2020 (1993)

- ¹⁸ N. A. J. M. Kleemans, I. M. A. Bominaar-Silkens, V. M. Fomin, V. N. Gladilin, D. Granados, A. G. Taboada, J. M. García, P. Offermans, U. Zeitler, P. C. M. Christianen, J. C. Maan, J. T. Devreese, and P. M. Koenraad, *Phys. Rev. Lett.* **99**, 146808 (2007)
- ¹⁹ C. Somaschini, S. Bietti, N. Koguchi, and S. Sanguinetti, *Nano Letters* **9**, 3419 (2009)
- ²⁰ R. Petta, A. C. Johnson, J. M. Taylor, E. A. Laird, A. Yacoby, M. D. Lukin, C. M. Marcus, M. P. Hanson, A. C. Gossard, *Science* **309**, 2180 (2005).
- ²¹ A. Kwasniowski and J. Adamowski, *J. Phys: Condens. Matter* **21**, 235601 (2009)
- ²² L.-X. Zhang, D. V. Melnikov, S. Agarwal, and J.-P. Leburton, *Phys. Rev. B* **78**, 035418 (2008).
- ²³ B. Szafran, F. M. Peeters, and S. Bednarek, *Phys. Rev. B* **70**, 125310 (2004)
- ²⁴ J. L. Gondar and F. Comas, *Physica B* **322**, 413 (2003).
- ²⁵ S. Yilmaz and H. Safak, *Physica E* **36**, 40 (2007).
- ²⁶ A. Özmen, Y. Yakar, B. Cakir and Ü. Atav, *Opt. Commun*, **282**, 3999 (2009).
- ²⁷ J. S. deSousa, J. P. Leburton, V. N. Freire, and E. F. daSilva, *Phys. Rev. B* **72**, 155438 (2005).
- ²⁸ I. Karabulut and S. Baskoutas, *J. Appl. Phys* **103**, 073512 (2008).
- ²⁹ M. Sahin, *Phys. Rev. B* **77**, 045317 (2008).
- ³⁰ A. Harju, S. Siljamäki, and R. M. Nieminen, *Phys. Rev. Lett.* **88**, 226804 (2002).
- ³¹ A. Patanè, N. Mori, O. Makarovskiy, L. Eaves, M. L. Zambrano, J. C. Arce, L. Dickinson, and D. K. Maude, *Phys. Rev. Lett.* **105**, 236804 (2010).
- ³² S. Kais y P. Serra, *Adv. Chem. Phys.* **125**, 1 (2003).
- ³³ G.W. Bryant, *Phys. Rev. B* **52**, R16997 (1995)
- ³⁴ R. Buczko and F. Bassani, *Phys. Rev. B* **54**, 2667 (1996)
- ³⁵ S. Bednarek, B. Szafran, K. Lis, and J. Adamowski, *Phys. Rev. B* **68**, 155333 (2003)